doi:10.1093/brain/awx044 BRAIN 2017: 140; 1420–1436 | 1420

BRAIN
A JOURNAL OF NEUROLOGY

Insulin resistance and exendin-4 treatment for multiple system atrophy

Fares Bassil,[1,2] Marie-Hélène Canron,[1,2] Anne Vital,[1,2,3] Erwan Bezard,[1,2] Yazhou Li,[4] Nigel H. Greig,[4] Seema Gulyani,[5] Dimitrios Kapogiannis,[5] Pierre-Olivier Fernagut[1,2] and Wassilios G. Meissner[1,2,6,7]

See Stayte and Vissel (doi:10.1093/awx064) for a scientific commentary on this article.

Multiple system atrophy is a fatal sporadic adult-onset neurodegenerative disorder with no symptomatic or disease-modifying treatment available. The cytopathological hallmark of multiple system atrophy is the accumulation of α-synuclein aggregates in oligodendrocytes, forming glial cytoplasmic inclusions. Impaired insulin/insulin-like growth factor-1 signalling (IGF-1) and insulin resistance (i.e. decreased insulin/IGF-1) have been reported in other neurodegenerative disorders such as Alzheimer's disease. Increasing evidence also suggests impaired insulin/IGF-1 signalling in multiple system atrophy, as corroborated by increased insulin and IGF-1 plasma concentrations in multiple system atrophy patients and reduced IGF-1 brain levels in a transgenic mouse model of multiple system atrophy. We here tested the hypothesis that multiple system atrophy is associated with brain insulin resistance and showed increased expression of the key downstream messenger insulin receptor substrate-1 phosphorylated at serine residue 312 in neurons and oligodendrocytes in the putamen of patients with multiple system atrophy. Furthermore, the expression of insulin receptor substrate 1 (IRS-1) phosphorylated at serine residue 312 was more apparent in inclusion bearing oligodendrocytes in the putamen. By contrast, it was not different between both groups in the temporal cortex, a less vulnerable structure compared to the putamen. These findings suggest that insulin resistance may occur in multiple system atrophy in regions where the neurodegenerative process is most severe and point to a possible relation between α-synuclein aggregates and insulin resistance. We also observed insulin resistance in the striatum of transgenic multiple system atrophy mice and further demonstrate that the glucagon-like peptide-1 analogue exendin-4, a well-tolerated and Federal Drug Agency-approved antidiabetic drug, has positive effects on insulin resistance and monomeric α-synuclein load in the striatum, as well as survival of nigral dopamine neurons. Additionally, plasma levels of exosomal neural-derived IRS-1 phosphorylated at serine residue 307 (corresponding to serine residue 312 in humans) negatively correlated with survival of nigral dopamine neurons in multiple system atrophy mice treated with exendin-4. This finding suggests the potential for developing this peripheral biomarker candidate as an objective outcome measure of target engagement for clinical trials with glucagon-like peptide-1 analogues in multiple system atrophy. In conclusion, our observation of brain insulin resistance in multiple system atrophy patients and transgenic mice together with the beneficial effects of the glucagon-like peptide-1 agonist exendin-4 in transgenic mice paves the way for translating this innovative treatment into a clinical trial.

1 Univ. de Bordeaux, Institut des Maladies Neurodégénératives, UMR 5293, 33000 Bordeaux, France
2 CNRS, Institut des Maladies Neurodégénératives, UMR 5293, 33000 Bordeaux, France
3 Service de Pathologie, CHU de Bordeaux, 33000 Bordeaux, France
4 Translational Gerontology Branch, Intramural Research Program, National Institute on Aging, Baltimore, MD 21224, USA
5 Laboratory of Neurosciences, National Institute on Aging, Baltimore, MD 21224, USA
6 Centre de Référence Maladie Rare AMS, Hôpital Pellegrin, CHU de Bordeaux, F-33076 Bordeaux, France
7 Service de Neurologie, Hôpital Pellegrin, CHU de Bordeaux, 33000 Bordeaux, France

Received September 22, 2016. Revised December 14, 2016. Accepted January 10, 2017. Advance Access publication March 14, 2017.

Correspondence to: Prof. Wassilios Meissner,
Institute of Neurodegenerative Diseases, University Bordeaux, 146 rue Léo Saignat, 33076
Bordeaux Cedex, France
E-mail: wassilios.meissner@chu-bordeaux.fr

Keywords: movement disorders; MSA; alpha-synuclein; neuroprotection

Abbreviations: GCI = glial cytoplasmic inclusion; MSA = multiple system atrophy; SNc = substantia nigra pars compacta

Introduction

Multiple system atrophy (MSA) is a sporadic adult-onset, rare neurodegenerative disorder clinically characterized by a variable combination of parkinsonism, cerebellar impairment and autonomic dysfunction (Gilman *et al.*, 2008). The cytopathological hallmark of MSA is the accumulation of α-synuclein aggregates in oligodendrocytes, forming glial cytoplasmic inclusions (GCIs) (Gilman *et al.*, 2008; Wenning *et al.*, 2008). There is currently no treatment available to mitigate symptom severity or clinical progression. Developing neuroprotective treatments for MSA is therefore an urgent unmet need (Fernagut *et al.*, 2014*a*).

Several studies have demonstrated impaired insulin/insulin-like growth factor-1 (IGF-1) signalling and insulin resistance (i.e. decreased insulin signalling) in neurodegenerative disorders, particularly in Alzheimer's disease (Bassil *et al.*, 2014). A measure of insulin resistance is the amount of the downstream messenger insulin receptor substrate-1 (IRS-1) phosphorylated at serine residues 312 (IRS-1pS312) or 616 (IRS-1pS616) (Moloney *et al.*, 2010; Talbot *et al.*, 2012). Increasing evidence suggests impaired insulin/IGF-1 signalling in MSA, as shown by increased insulin and IGF-1 plasma concentrations in MSA patients and reduced IGF-1 brain levels in a transgenic mouse model of MSA (Pellecchia *et al.*, 2010; Ubhi *et al.*, 2010; Numao *et al.*, 2014).

Insulin and IGF-1 sources are primarily peripheral, but they are also synthesized in the brain (Schechter *et al.*, 1996; Jafferali *et al.*, 2000). In the brain, insulin/IGF-1 signalling is involved in numerous biological processes including myelin sheath synthesis, astrocyte glycogen storage, cholesterol production, oligodendrogenesis and maturation, as well as neuronal survival. The effects of insulin and IGF-1 are mediated through IRS-1 and its downstream target Akt, which acts as a central hub modulating the activity of several effectors implicated in oxidative stress, apoptosis, protein synthesis, gene expression, autophagy and inflammation (Bassil *et al.*, 2014). These biological processes are altered and thought to be crucially involved in the pathogenesis of MSA (Nakamura *et al.*, 1998, 2001; Schwarz *et al.*, 1998; Kragh *et al.*, 2013; Bassil *et al.*, 2014; Fernagut *et al.*, 2014*a*).

Glucagon-like peptide-1 (GLP-1), an insulinotropic hormone, activates the same effectors as insulin and IGF-1. GLP-1 and its receptor (GLP-1R) are expressed in neurons and receptor activation has positive effects on cell proliferation, neurogenesis and apoptosis (Bassil *et al.*, 2014). Synthetic GLP-1 analogues such as exendin-4 are resistant to dipeptidyl peptidase-4, the main GLP-1 degrading enzyme. Exendin-4 crosses the blood–brain barrier, similar to GLP-1, and binds to the GLP-1R. GLP-1 analogues have positive effects on behaviour and surrogate markers of neurodegeneration in preclinical models of Alzheimer's disease and Parkinson's disease (Bassil *et al.*, 2014). These encouraging results have set the ground for translation into early clinical trials in Alzheimer's disease (NCT01255163, NCT01469351, NCT01843075) and Parkinson's disease (Aviles-Olmos *et al.*, 2013, 2014; Bassil *et al.*, 2014). The results of a small open-label phase 2 clinical trial evaluating the safety and efficacy of the GLP-1 agonist exendin-4 showed a significant improvement in motor scores and cognitive efficiency at 12 months in patients with Parkinson's disease treated with exendin-4 compared to a control group, which persisted following cessation of administration (Aviles-Olmos *et al.*, 2013, 2014).

Hence, if insulin resistance occurs in the brain in MSA, modulating insulin/IGF-1 signalling might provide an effective approach to disease modification. We thus tested the hypothesis that MSA is associated with brain insulin resistance and showed increased expression of IRS-1pS312 (corresponds to IRS-1pS307 in mice) in the putamen of MSA patients and transgenic MSA mice. We further demonstrated that exendin-4, a well-tolerated FDA-approved antidiabetic drug, has positive effects on cell survival, α-synuclein load, as well as central and peripheral markers of insulin resistance in transgenic MSA mice opening the way for translating this innovative treatment into a clinical trial in patients with MSA.

Materials and methods

Study approval

All experiments involving mice were performed in accordance with French guidelines (87-848, Ministère de l'Agriculture et de la Forêt) and the European Community Council Directive (2010/63/EU) for the care of laboratory animals. Animal experiments were approved by the Institutional Animal Care and Use Committee of Bordeaux (CE50, license #50120100-A). Mice were maintained in a temperature- and humidity-controlled room on a 12:12 light-dark cycle with food and water *ad libitum*. For the human post-mortem studies, informed consent was obtained for collection and use of clinical

and post-mortem data from all subjects of the study or from their family. Human brain samples were obtained from the GIE-Neuro CEB and the Bordeaux Brain Bank (DC-2014-2164).

Human brain samples

Formalin-fixed and paraffin-embedded material from the putamen and temporal cortex was available for the seven neuropathologically confirmed MSA cases and the five control subjects. The putamen and temporal cortex were studied within coronal 4-µm thick sections demonstrating the lentiform nucleus. Characteristics of MSA patients and healthy controls are given in Table 1. Mean age was not different between groups (control: 63.8 ± 5.7 years and MSA: 67.4 ± 3.7 years, $P = 0.34$). According to the clinical records, none of the assessed subjects had a diagnosis of diabetes at the time of death. No data of fasting blood glucose and insulin concentrations close to death were available to formally exclude peripheral insulin resistance.

Animals

Mice expressing human α-synuclein in oligodendrocytes under the control of the proteolipid promoter (PLP-SYN) were previously generated on a C57BL/6 background (Kahle *et al.*, 2002). The study was conducted in three separate sets of animals. The first was used to determine brain insulin resistance in PLP-SYN mice ($n = 7$) and wild-type littermates ($n = 7$). In the second set, PLP-SYN ($n = 25$) mice aged 6 weeks were used to study the effects of exendin-4 treatment. PLP-SYN mice were randomly allocated into three groups: placebo ($n = 9$), exendin-4 at 3.5 pmol/kg/min ($n = 9$), and exendin-4 at 8.75 pmol/kg/min ($n = 7$). After 12 weeks of treatment, motor behaviour was evaluated before euthanizing the animals. The third set was used to measure exendin-4 plasma levels at steady state in animals treated with 3.5 pmol/kg/min ($n = 6$) or 8.75 pmol/kg/min ($n = 7$). Plasma exosomal neural-derived levels of IRS-1pS307 were further determined in mice treated with 8.75 pmol/kg/min ($n = 7$).

Pharmacological treatment

Exendin-4 (Catalogue number: 228-10419-3, Tebu-bio SAS) was diluted in 0.9% sterile saline and delivered subcutaneously via Alzet osmotic minipumps (Model 1004). The two doses of exendin-4, delivered at a rate of 3.5 pmol/kg/min or 8.75 pmol/kg/min, are of translational relevance. Following normalization of body surface area between mouse and humans, the higher dose compares favourably to the clinical dose of the once weekly form of exendin-4 (Bydureon®) used in type 2 diabetes (FDA, 2005). The same vehicle without exendin-4 was administered to the placebo group. In all animals, pumps were placed subcutaneously, posterior to the scapulae (Li *et al.*, 2009). Every 4 weeks, pumps were replaced with freshly prepared exendin-4 (adjusted to the diffusion rate and average weight of the group) or saline until the completion of the 12-week study. Mean plasma levels were 2197.6 ± 317.7 pg/ml for PLP-SYN mice treated with 3.5 pmol/kg/min ($n = 6$) and 2796.3 ± 284.9 pg/ml for those receiving 8.5 pmol/kg/min ($n = 7$). Plasma levels of exendin-4 were quantified by using the Exendin-4 Chemiluminescent Enzyme Immunoassay Kit (Phoenix Pharmaceuticals Inc.). Each mouse plasma sample was measured in duplicate in the volume of 50 µl each without dilution. The final results are all in the linear range of the standard curve.

Behavioural test

Motor coordination and balance were assessed with the challenging traversing beam task as previously described (Fleming *et al.*, 2004; Fernagut *et al.*, 2007, 2014*b*). This test measures the ability of the mouse to traverse a narrowing beam to reach its home cage and is the most sensitive test to assess motor function in PLP-SYN mice (Fernagut *et al.*, 2014*b*).

Tissue processing and plasma extraction

At the end of the 12-week treatment period, mice were anaesthetized with pentobarbital (100 mg/kg intraperitoneally).

Table 1 Demographic data, post-mortem delay and disease duration of assessed subjects

Subject	MSA subtype	Age	Sex	Post-mortem delay (h)	Disease duration (years)
Control	–	54	F	<48	–
Control	–	84	F	16	–
Control	–	69	M	<48	–
Control	–	55	M	<48	–
Control	–	57	M	<48	–
MSA	P	73	F	24	3
MSA	NA	57	F	24	2
MSA	P	57	F	7	7
MSA	Mixed	59	M	24	8
MSA	P	83	F	12	6
MSA	P	71	F	24	3
MSA	P	72	M	48	6

Patients with MSA, $n = 7$; control subjects, $n = 5$.
F = female; M = male; P = predominant parkinsonism; NA = not available.

Blood was collected directly from the heart into EDTA tubes (2 ml) and centrifuged at 5000 rpm for 15 min at 4°C for plasma collection. After blood sampling, mice were intracardially perfused with 0.9% saline. Brains were quickly removed and cut in half between the two hemispheres. The right hemisphere was frozen directly for biochemical analysis while the left hemisphere was post-fixed for 5 days in 4% paraformaldehyde.

Immunoblotting

Striatal tissue extracts of mice were prepared as previously described (Dehay *et al.*, 2010). To measure α-synuclein, proteins were loaded, run on 4–15% gradient gels (Bio-Rad) and transferred onto nitrocellulose membranes (Millipore). Membranes were incubated with human-specific antibody Syn-211 (1:1000, Thermo Fisher Scientific), probed with the corresponding secondary antibody (1:2000, Jackson laboratories), visualized with enhanced chemiluminescence and analysed using the ChemiDoc™ gel imaging system (Bio-Rad). To assess insulin resistance, the same protocol was used using 8% SDS-PAGE gels and antibodies against insulin resistance markers IRS-1pS307 (rabbit polyclonal antibody, 1:2000; Invitrogen) or IRS-1pS612 (corresponds to IRS-1pS616 in humans; rabbit polyclonal antibody, 1:2000, Invitrogen). Proteins were normalized to actin (1:2000, Sigma), used as a loading control.

Histopathological analysis and immunofluorescent labelling

Sequential immunofluorescence labelling was performed on 4-µm thick paraffin-embedded putamen and temporal cortex sections from MSA patients and controls. Following antigen retrieval with citrate buffer pH6 (Dako), sections were probed for IRS-1pS312 (rabbit polyclonal antibody, 1:200, Invitrogen) or IRS-1pS616 (rabbit polyclonal antibody, 1:200, Invitrogen) coupled to either the anti-glial fibrillary acidic protein (GFAP, mouse monoclonal antibody, 1:500, Millipore) combined with S100β (mouse monoclonal antibody, 1:1000, Abcam), the microglial marker anti-HLA-DR (mouse monoclonal antibody, clone TAL.1B5, 1:500, Dako), the oligodendrocyte marker anti-2',3'-cyclic-nucleotide 3'-phosphodiesterase (CNPase, mouse monoclonal antibody, clone 11-5B, 1:500, Abcam) or the neuronal marker anti-microtubule-associated protein 2 (MAP-2, mouse monoclonal antibody, clone AP20, 1:500, Millipore). Thereafter, sections were incubated with the appropriate secondary antibody (Invitrogen). Slides were then incubated with 0.1% Sudan Black B (Sigma-Aldrich) in 70% ethanol to lower the intensity of lipofuscin auto-fluorescence.

For the assessment of a possible relation between α-synuclein aggregates and insulin resistance in oligodendrocytes, sections were sequentially incubated with the oligodendrocyte marker anti-CNPase (chicken polyclonal antibody, 1:100, Abcam; revealed with goat anti-chicken Alexa 647, 1:200, Abcam), followed by IRS-1pS312 (rabbit polyclonal antibody, 1:200, Invitrogen; revealed with donkey anti-rabbit Alexa 568, 1:400, Invitrogen), then α-synuclein (mouse monoclonal antibody, clone LB509, 1:100, Life Technology; revealed with goat anti-mouse Alexa 488, 1:400, Invitrogen). Slides were then incubated with 0.1% Sudan Black B (Sigma-Aldrich) in 70% ethanol to lower the intensity of lipofuscin autofluorescence. Nuclei were counterstained with DAPI.

For mouse studies, 40 µm free-floating coronal sections were collected for histopathological analysis and every fourth section was processed for tyrosine hydroxylase (TH) immunohistochemistry and counterstained with cresyl violet as previously described (Fernagut *et al.*, 2014*b*).

Quantitative analysis

Analysis of the number of immunopositive cells was performed using a computerized image analysis system (Morphostrider, Explora Nova) linked to a Zeiss fluorescence microscope Imager M2. For co-localization analysis, nine images were taken randomly from MSA patients and healthy controls at ×40 magnification, and image analysis was undertaken using ImageJ v1.47 implemented with the co-localization threshold plugin. A threshold was applied to all images in green (MAP-2, HLA-DR, CNPase, GFAP/S100β and α-synuclein) and another was used for the red (IRS-1pS312, IRS-pS616, and CNPase for the assessment of a possible relation between α-synuclein aggregates and insulin resistance in oligodendrocytes) filter to assess co-localization. To assess IRS-1pS312 levels depending on the presence of GCI, oligodendrocytes were first identified based on CNPase and DAPI staining. CNPase/α-synuclein overlay was used to discriminate between GCI-positive and GCI-negative oligodendrocytes, then IRS-1pS312 intensity was measured in each identified oligodendrocyte.

The intensity of IRS-1pS312- and IRS-1pS616-positive cells was measured and values were determined according to cell type. For cell fluorescence intensity, ImageJ software was used to measure pixel intensity and area with respect to background intensity and cell surface, respectively, according to the following formula: Intensity of stained cell − (sample of background/area of sample background) × area of stained cell. To minimize the inherent variability in the immunofluorescence procedure, sections from all cases were processed simultaneously for a given marker.

For TH and Nissl counts in the substantia nigra pars compacta (SNc), stereological sampling was performed using the Mercator Pro V6.5 software (Explora Nova) coupled to a Leica DM-6000B microscope with a motorized XYZ stage (Fernagut *et al.*, 2014*b*). Following delineation of the SNc at 5× objective as described previously (Fernagut *et al.*, 2007, 2014*b*) counting was performed at 63× objective.

Measurement of plasma neural derived exosomal IRS-1pS307 in transgenic mice

Plasma samples (50 µl) were assessed from the mice treated with 8.5 pmol/kg/min for 12 weeks ($n = 7$). Samples were obtained at the time of their sacrifice. For detailed description of the methods for enriching plasma extracellular vesicles for neuronal origin by means of L1CAM immunoprecipitation, we refer to previous publications (Fiandaca *et al.*, 2015; Goetzl *et al.*, 2015; Kapogiannis *et al.*, 2015). Briefly, ExoQuick™ exosome solution (System Biosciences) was used to precipitate total exosomes. Each exosome pellet was resuspended in 150 µl distilled water with inhibitor cocktails before immunochemical enrichment of exosomes from neural sources. Each exosome suspension was incubated for 1 h at 4°C with 1 µg mouse anti-CD171

(L1CAM) biotinylated antibody (clone 5G3; eBioscience) in 50 µl 3% bovine serum albumin (BSA; 1:3.33 dilution of blocker BSA 10% solution in DBS-2; Thermo Fisher Scientific), followed by addition of 25 µl streptavidin-agarose resin (Thermo Fisher Scientific) with 50 µl 3% BSA and incubation for 30 min at 4°C. After centrifugation at 200*g* for 10 min at 4°C and removal of the supernatant, each pellet was suspended in 50 µl 0.05 M glycine-HCl (pH3.0) by vortexing for 10 s. Each suspension then received 0.5 ml M-PER mammalian protein extraction reagent (Thermo Fisher Scientific) that had been adjusted to pH8.0 with 1 M Tris-HCl (pH8.6) and contained the cocktails of protease and phosphatase inhibitors. These suspensions were incubated at 37°C for 10 min and vortex-mixed for 15 s before storage at −80°C. After single thaw, IRS-1pS307 protein was quantified by electrochemiluminescence using the commercially available Mesoscale discovery kit (MSD-K150HLD-2). The exosomal marker alix was quantified by a custom-made electrochemiluminescence assay akin to sandwich ELISA using biotin conjugated mouse monoclonal anti-alix (Abcam 117600) as a capture antibody and rabbit polyclonal anti-alix (Abcam 104256) as a detection antibody. The assay was developed on a 96-well streptavidin coated plate (MSD-L15SA1). Briefly, plates were coated with capture antibody overnight followed by incubation with samples for 1 h. After the incubation plates were washed and incubated with detection antibody mixed along with MSD-sulfo tag labelled anti-rabbit antibody (R32AB-1). Plates were washed again and after electrochemiluminescence reaction on the MSD platform, signal was read using MSD software. A standard curve was obtained using a full-length recombinant protein (Abcam 132534) with concentrations ranging from 25 pg/ml to 40 µg/ml. Standards were diluted in the same lysis buffer used for L1CAM and exosome samples. The lower level of detection was defined as the concentration of the standard that provided signal higher than the mean of the blank plus 9 times the standard deviation of the blank, showed a coefficient of variance <20% among replicates and a recovery of the known concentration between 80 and 120%. The lower level of detection for the alix assay was determined to be 62 ng/ml. The samples ranged in the concentrations from 300 ng/ml to 10 µg/ml. All the samples were in the linear range of the standard curve. Concentrations of IRS-1pS307 were normalized by alix.

Statistics

For the comparison between two groups, a *t*-test was applied. If data were not normally distributed, a Mann-Whitney test was used instead. A one-way ANOVA was applied to compare treatment effects of exendin-4 between groups on behaviour, striatal IRS-1pS307/IRS-1pS612 protein levels, striatal α-synuclein protein expression, as well as TH and Nissl counts, followed by *post hoc* Holm-Sidak tests for multiple comparisons if appropriate. For *post hoc* comparisons of striatal IRS-1pS307/IRS-1pS612 protein and α-synuclein protein levels, PLP-SYN placebo mice were defined as control group. If data were not normally distributed, an ANOVA on ranks was performed instead, followed by Dunn's multiple comparisons when appropriate. Correlation analysis was performed by calculating the Pearson correlation coefficient between the staining intensity of IRS-1pS312 in neurons and oligodendrocytes, age, post-mortem delay and disease duration. In transgenic mice, the Pearson correlation coefficient was calculated for neural-derived exosomal IRS-1pS307 concentrations and striatal α-synuclein protein levels, as well as TH and Nissl counts. Statistical analysis was performed with Sigmaplot 12 software (Systat Software Inc.). Data are presented as mean ± standard error of the mean (SEM). Statistical tests were two-tailed and the level of significance was set at $P < 0.05$.

Results

Neurons are insulin resistant in multiple system atrophy

Using immunofluorescence staining with the neuronal marker MAP-2, we quantified the number of neurons immunopositive for the insulin resistance markers IRS-1pS312 and IRS-1pS616 in the putamen of both MSA patients and healthy controls (Fig. 1A, B, E and F). Co-localization analysis revealed that virtually all neurons expressed IRS-1pS312 and IRS-1pS616.

As a result of severe striatal neuronal loss, patients with MSA showed a significant decrease in the number of MAP-2-positive neurons compared to healthy controls in the putamen (MSA, 106.8 ± 19.6/mm^2; controls, 298.5 ± 26.4/mm^2; $P < 0.001$) (Salvesen *et al.*, 2015). Accordingly, the numbers of IRS-1pS312 ($P < 0.001$) and IRS-1pS616 ($P < 0.001$) positive neurons were decreased in MSA patients compared to healthy controls (Fig. 1A–C and E–G).

We then measured the fluorescence intensity of insulin resistance markers in neurons of MSA patients and healthy subjects. IRS-1pS312 staining intensity was significantly increased in surviving neurons of MSA patients compared to healthy subjects (+82%, $P < 0.01$, Fig. 1D). The localization of IRS-1pS312 in neurons of MSA patients and controls was nuclear. The intensity of neuronal IRS-1pS312 staining was positively correlated with disease duration ($\rho = 0.86$, $P < 0.05$). IRS-1pS616 staining showed also a trend for higher intensity in MSA patients compared to healthy controls (+141%, $P = 0.15$, Fig. 1H).

We then assessed the temporal cortex, a structure where neuropathological changes are mild in MSA (Papp and Lantos, 1994). Interestingly, the intensity of neuronal IRS-1pS312 staining was not different between MSA patients and controls in this region (Supplementary Fig. 1).

Oligodendrocytes are insulin resistant in multiple system atrophy

As MSA is pathologically characterized by the presence of GCIs, we next investigated insulin resistance in oligodendrocytes. Cell counts of CNPase positive oligodendrocytes were similar between groups (MSA, 281.2 ± 32.7/mm^2; controls, 280.4 ± 36.9/mm^2) and in accordance with previous results (Ettle *et al.*, 2016). Double immunofluorescence showed that virtually all oligodendrocytes stained positive for IRS-1pS312 and IRS-1pS616 (Fig. 2A, B, E and F). Accordingly, no significant differences were found between groups regarding the number of IRS-

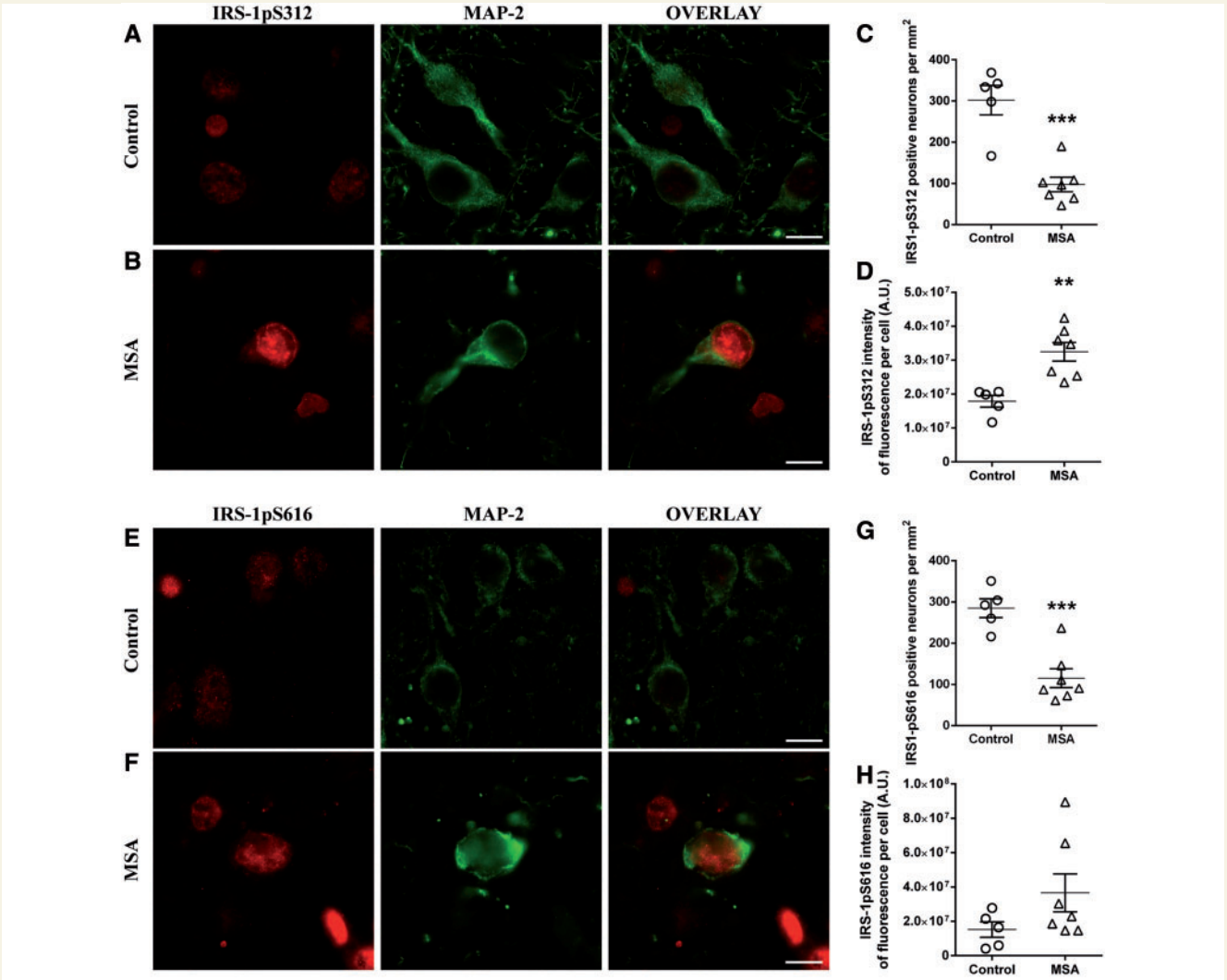

Figure 1 Neurons are insulin resistant in MSA. Representative images of IRS-1pS312 and IRS-1pS616 staining in neurons of controls ($n = 5$) (**A** and **E**) and MSA patients ($n = 7$) (**B** and **F**). The number of IRS-1pS312 and IRS-1pS616 positive neurons is decreased in MSA ($n = 7$) compared to healthy controls ($n = 5$) (**C** and **G**). IRS-1pS312 staining intensity is increased in neurons of MSA patients ($n = 7$) compared to healthy controls ($n = 5$) (**D**), while no differences were observed for IRS-1pS616 staining intensity (**H**). Scale bar = 10 μm. A *t*-test was used to compare data between MSA patients and healthy controls. If data were not normally distributed, a Mann-Whitney test was used instead. Values are mean ± SEM. $^{**}P < 0.01$ and $^{***}P < 0.001$ versus controls. A.U. = arbitrary units.

1pS312 or IRS-1pS616 positive oligodendrocytes (Fig. 2A–C and E–G). Interestingly, the intensity of IRS-1pS312 staining in CNPase positive oligodendrocytes was significantly increased in MSA patients compared to healthy controls (+90%, $P < 0.05$, Fig. 2D), whereas no difference was found in IRS-1pS616 intensity between the two groups (Fig. 2H). The localization of IRS-1pS312 in oligodendrocytes of MSA patients and controls was nuclear. The intensity of oligodendroglial IRS-1pS312 staining was negatively correlated with disease duration ($\rho = -0.87$, $P < 0.05$) and there was also an inverse relation between neuronal and oligodendroglial IRS-1pS312 staining intensity ($\rho = -0.84$, $P < 0.05$).

We then assessed whether IRS-1pS312 expression is more apparent in α-synuclein containing oligodendrocytes in MSA patients. Indeed, the staining intensity of IRS-1pS312 was higher in GCI containing oligodendrocytes (+61 ± 15%, $P < 0.01$) compared to those without α-synuclein aggregates in all MSA patients (Supplementary Fig. 2).

Similar to neurons, the intensity of oligodendroglial IRS-1pS312 staining in the temporal cortex was not different between MSA patients and controls (Supplementary Fig. 1).

Microglia and astrocyte IRS-1pS312 levels are unchanged in multiple system atrophy

Neuronal loss in MSA was accompanied by increased GFAP-positive astrocytes compared to healthy controls (MSA, 228.9 ± 21.4/mm^2; controls, 114.4 ± 10.5/mm^2; $P < 0.01$), as previously described (Salvesen *et al.*, 2015).

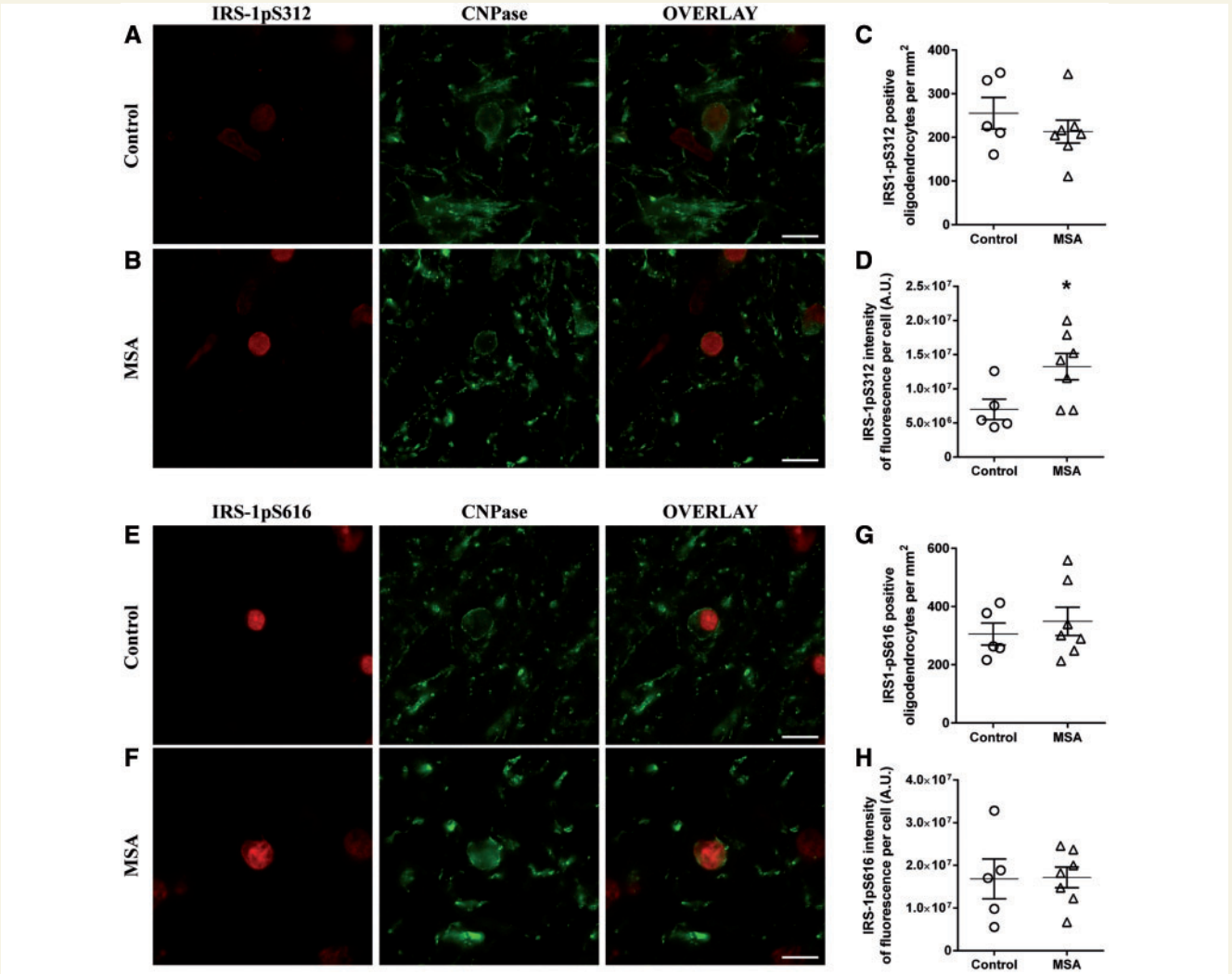

Figure 2 Oligodendrocytes are insulin resistant in MSA. Representative images of IRS-1pS312 and IRS-1pS616 staining in oligodendrocytes of controls ($n = 5$) (**A** and **E**) and MSA patients ($n = 7$) (**B** and **F**). The number of IRS-1pS312 and IRS-1pS616 positive oligodendrocytes was similar in both groups (**C** and **G**). IRS-1pS312 staining intensity is increased in oligodendrocytes of MSA patients ($n = 7$) compared to healthy controls ($n = 5$) (**D**). Quantification of IRS-1pS616 staining intensity showed no significant difference between groups (**H**). Scale bar = 10 μm. A *t*-test was used to compare data between MSA patients and healthy controls. If data were not normally distributed, a Mann-Whitney test was used instead. Values are mean ± SEM. *$P < 0.05$ versus controls. A.U. = arbitrary units.

Co-localization analysis showed that almost all astrocytes stained positive for IRS-1pS312 and IRS-1pS616 (Fig. 3A, B, E and F). Accordingly, the numbers of IRS-1pS312 ($P < 0.01$) and IRS-1pS616 ($P < 0.01$) positive astrocytes were increased in MSA compared to healthy subjects (Fig. 3A–C and E–G). IRS-1pS312 staining intensity was not different between groups (Fig. 3D), while a trend for a decrease was observed for IRS-1pS616 staining intensity in astrocytes ($P = 0.09$, Fig. 3H).

MSA patients also showed increased HLA-DR positive microglia compared to healthy controls (MSA, $82.4 \pm 16.6/mm^2$; controls, $38.9 \pm 7.1/mm^2$; $P < 0.05$), as previously described (Salvesen *et al.*, 2015). IRS-1pS312 and IRS-1pS616 co-localized with HLA-DR staining in almost all microglial cells (Fig. 4A, B, E and F). Accordingly, the number of IRS-1pS312 and IRS-1pS616 positive microglial cells was higher in the putamen of MSA patients compared to healthy controls (Fig. 4A–C and E–G). However, these differences were not significant (IRS-1pS312, $P = 0.09$; IRS-1pS616, $P = 0.11$). Staining intensity was not different between groups for IRS-1pS312 and IRS-1pS616 (Fig. 4D and H).

Phosphorylation of IRS-1 in the brain is a dynamic process that might be affected by several parameters, most notably aging and post-mortem delay. Statistical analysis showed no correlation between age, post-mortem delay and IRS-1pS312 staining intensity in neurons and oligodendrocytes within each group.

Altogether these data indicate that insulin resistance, as measured by increased IRS-1p312 intensity, occurs in

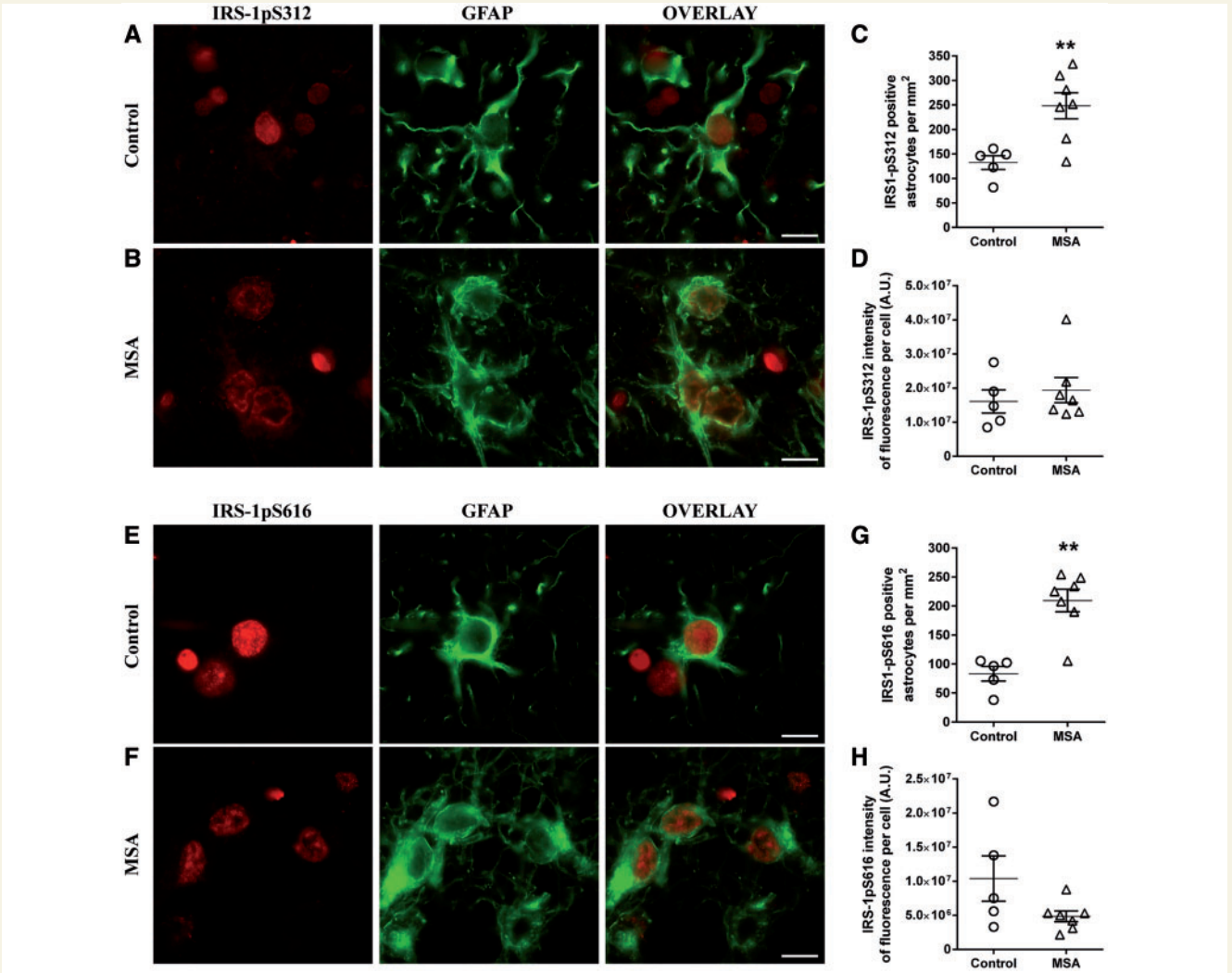

Figure 3 IRS-1pS312 and IRS-1pS616 staining intensity is not different in astrocytes. Representative images of IRS-1pS312 and IRS-1pS616 staining in astrocytes of controls ($n = 5$) (**A** and **E**) and MSA patients ($n = 7$) (**B** and **F**). The number of IRS-1pS312 and IRS-1pS616 positive astrocytes is increased in MSA patients ($n = 7$) compared to healthy controls ($n = 5$) (**C** and **G**). Quantification of IRS-1pS312 and IRS-1pS616 staining intensity showed no significant differences between groups (**D** and **H**). Scale bar = 10 μm. A *t*-test was used to compare data between MSA patients and healthy controls. If data were not normally distributed, a Mann-Whitney test was used instead. Values are mean ± SEM. $^{**}P < 0.01$ versus controls. A.U. = arbitrary units.

putaminal neurons and oligodendrocytes of MSA patients but not in astrocytes or microglial cells.

Insulin resistance occurs in the brain of transgenic multiple system atrophy mice

The PLP-SYN transgenic mouse model of MSA replicates several major features of human MSA (Kahle *et al.*, 2002; Fernagut and Tison, 2012). In light of our discovery of brain insulin resistance in MSA, we evaluated levels of IRS-1pS307 (corresponding to human IRS-1pS312) and IRS-1pS612 (corresponding to human IRS-1pS616) in the striatum of PLP-SYN mice. The expression of the insulin resistance marker IRS-1pS307 was significantly increased compared to wild-type littermates (+118%, $P < 0.01$, Fig. 5A and B), a result in agreement with increased IRS-1pS312 intensity in remaining neurons and oligodendrocytes in MSA patients. IRS-1pS612 showed a trend toward elevated levels in the striatum of PLP-SYN mice compared to wild-type littermates (+33%, $P = 0.09$, Fig. 5C and D).

Positive effects of exendin-4 on insulin resistance and cell death but not on motor signs in multiple system atrophy mice

As PLP-SYN mice were insulin-resistant, we then examined the effect of the GLP-1 agonist exendin-4 on levels of IRS-1pS307 and IRS-1pS612. Six-week-old PLP-SYN mice were

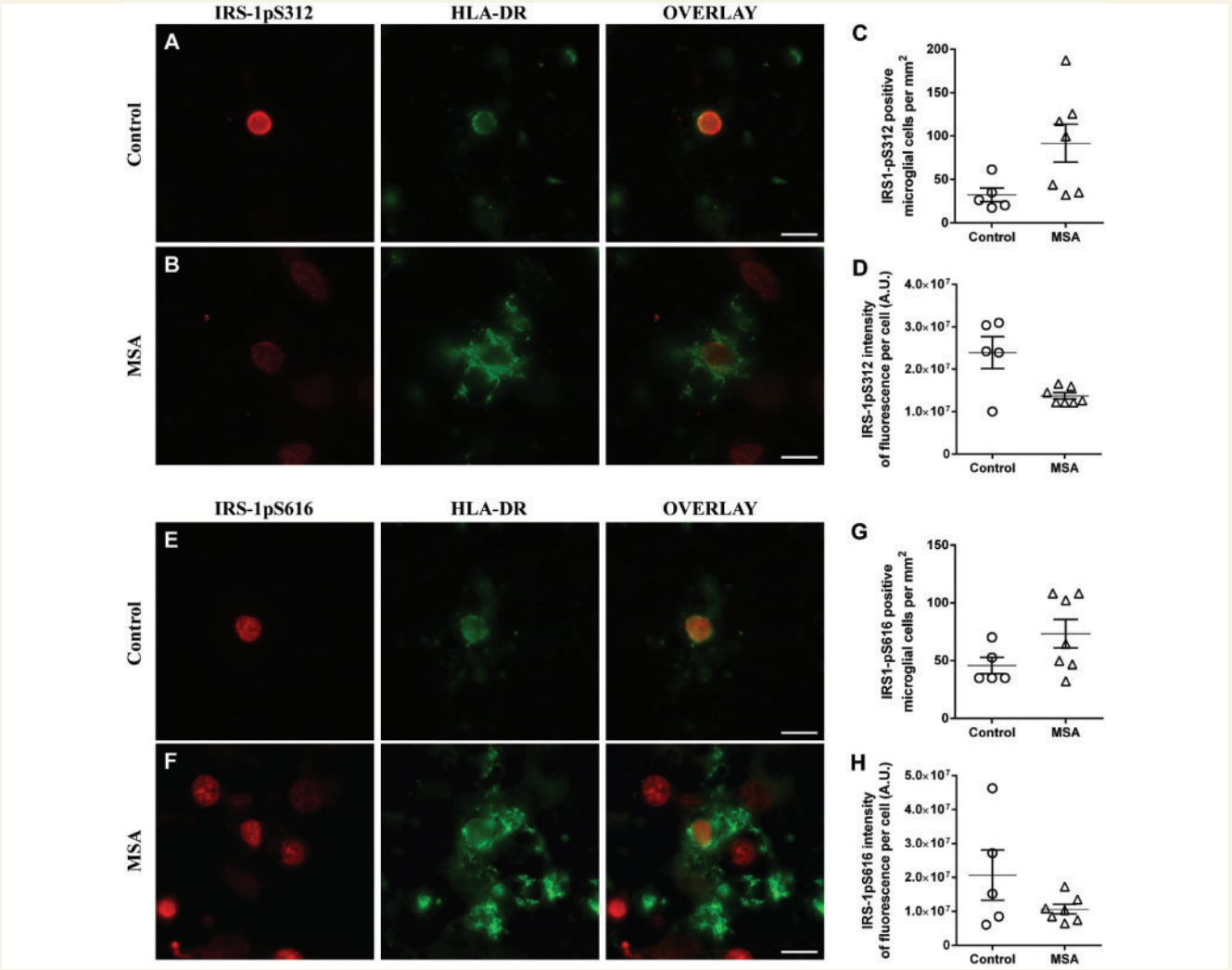

Figure 4 IRS-1pS312 and IRS-1pS616 staining intensity is not different in microglia. Representative images of IRS-1pS312 and IRS-1pS616 staining in microglia of controls ($n = 5$) (**A** and **E**) and MSA patients ($n = 7$) (**B** and **F**). The number of IRS-1pS312 and IRS-1pS616 positive microglia is not different in MSA patients ($n = 7$) compared to healthy controls ($n = 5$) (**C** and **G**). IRS-1pS312 and IRS-1pS616 staining intensity was not different between groups (**D** and **H**). Scale bar = 10 μm. A *t*-test was used to compare data between MSA patients and healthy controls. If data were not normally distributed, a Mann-Whitney test was used instead. Values are mean ± SEM. A.U. = arbitrary units.

treated for 12 weeks with exendin-4. Mice were separated into three groups receiving either placebo or exendin-4: 3.5 pmol/kg/min (lower dose) or 8.75 pmol/kg/min (higher dose). An overall comparison between groups showed that exendin-4 treatment had a significant effect on the expression of insulin resistance markers in PLP-SYN mice [IRS-1pS307: $F(2,24) = 3.7$, $P < 0.05$; IRS-1pS612: $H = 14.7$, $df = 2$, $P < 0.001$, Fig. 5E–H]. Specifically, *post hoc* analysis revealed a significant effect of the higher dose of exendin-4 treatment on IRS-1pS307 and IRS-1pS612 levels in PLP-SYN mice compared to placebo (IRS-1pS307: −36%, $P < 0.05$; IRS-1pS612: −42%, $P < 0.001$). Lower dose exendin-4 treatment had no effect on IRS-1pS307 or IRS-1pS612 levels.

Consequent to the success of exendin-4 treatment in ameliorating insulin resistance, we assessed whether it might also beneficially impact behaviour and overall pathology in these PLP-SYN mice. Transgenic MSA PLP-SYN mice display progressive motor impairment with ageing, as evidenced by an increased number of errors on the traversing beam task (Fernagut *et al.*, 2014*b*). A trend for improvement of motor performance in the traversing beam task was observed in PLP-SYN mice receiving the higher dose exendin-4 treatment but the difference between groups did not reach significance ($H = 3.8$, $df = 2$, $P = 0.15$, Fig. 6A).

PLP-SYN mice classically also show a loss of TH-positive neurons in the SNc, similar to MSA patients (Papp and Lantos, 1994; Ozawa *et al.*, 2004; Stefanova *et al.*, 2005; Fernagut *et al.*, 2014*b*). We thus evaluated the therapeutic efficacy of exendin-4 on TH-positive neuron survival within the SNc (Fig. 6B and D–F). A one-way ANOVA revealed significant differences between groups in dopaminergic cell counts in the SNc [$F(2,24) = 3.9$, $P < 0.05$]. A *post hoc* analysis revealed a significant preservation of dopaminergic

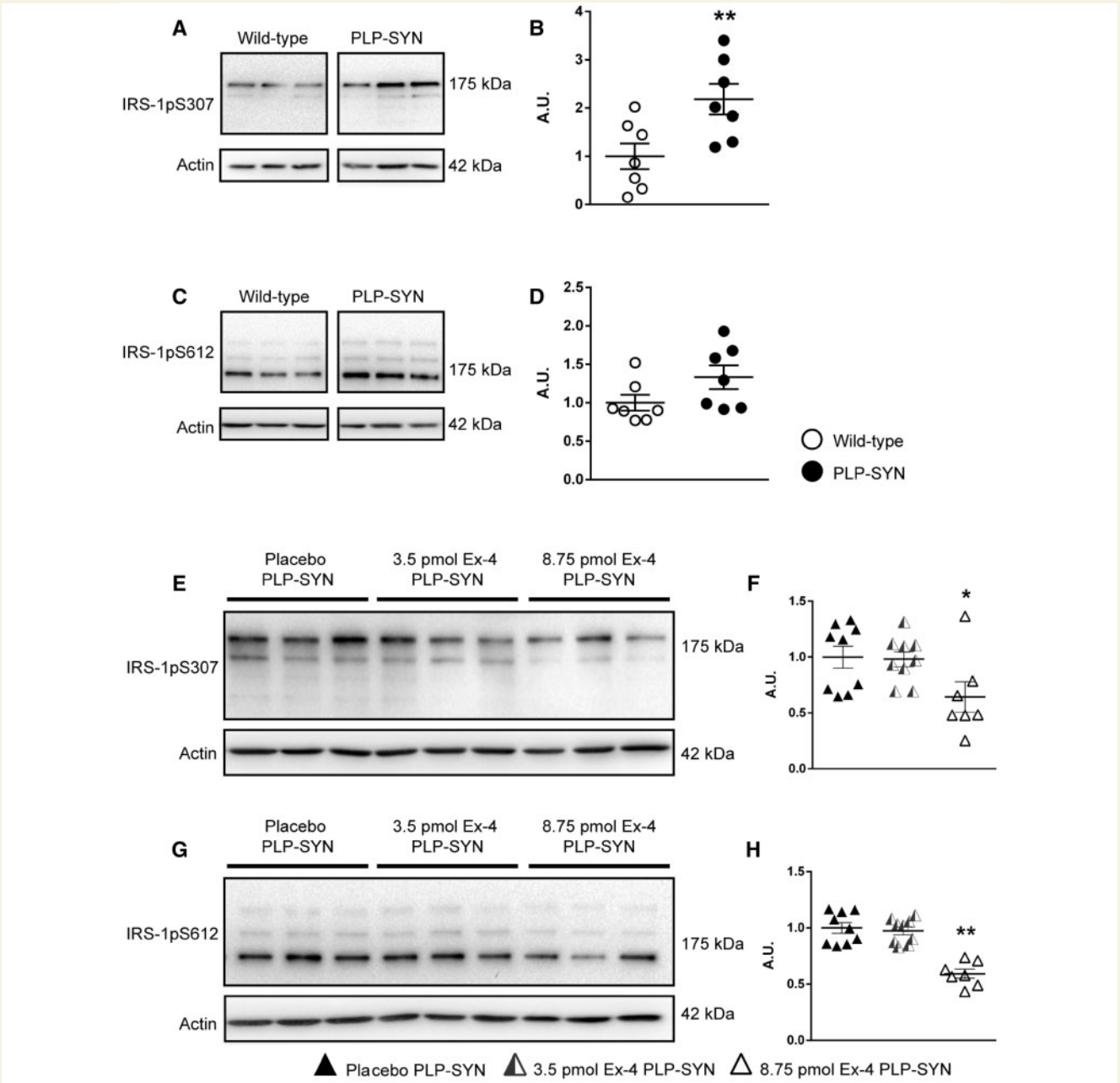

Figure 5 Insulin resistance in PLP-SYN mice is reversed by exendin-4 treatment. (**A**) Representative image of IRS-1pS307 protein levels in the striatum of PLP-SYN mice and wild-type littermates. (**B**) Significant increase in striatal IRS-1pS307 protein levels in PLP-SYN mice ($n = 7$) compared to wild-type (WT) littermates ($n = 7$). (**C**) Representative image of striatal IRS-pS612 protein expression levels in the striatum of PLP-SYN mice and wild-type littermates. (**D**) No difference was observed in IRS-1pS612 protein levels between groups. (**E** and **G**) Representative images of IRS-1pS307 and IRS-1pS612 protein expression in the striatum of PLP-SYN mice treated with placebo ($n = 9$), 3.5 pmol/kg/min ($n = 9$) or 8.75 pmol/kg/min exendin-4 ($n = 7$). (**F** and **H**) Significant decrease in IRS-1pS307 and IRS-1pS612 protein expression in the 8.75 pmol/kg/min exendin-4 treated group ($n = 7$) compared to placebo PLP-SYN mice ($n = 9$). A *t*-test was used to compare striatal IRS-1pS307 and IRS-1pS612 protein expression levels between PLP-SYN and wild-type littermates. A one-way ANOVA was applied to compare treatment effects of exendin-4 between groups, followed by *post hoc* Holm-Sidak tests for multiple comparisons if appropriate. If data were not normally distributed, an ANOVA on ranks was performed instead, followed by Dunn's multiple comparisons when appropriate. Values are mean ± SEM. *$P < 0.05$ versus placebo PLP-SYN, **$P < 0.01$ versus placebo PLP-SYN. A.U. = arbitrary units.

neurons in the SNc of PLP-SYN mice treated with the higher dose of exendin-4 compared to placebo PLP-SYN mice (+123%, $P < 0.05$ respectively, Fig. 6B and D–F). No significant effect of the lower dose of exendin-4 on dopaminergic neuron survival in PLP-SYN mice was observed (Fig. 6B and D–F).

We then confirmed our results by counting the number of Nissl stained neurons in the SNc. A Kruskal-Wallis test

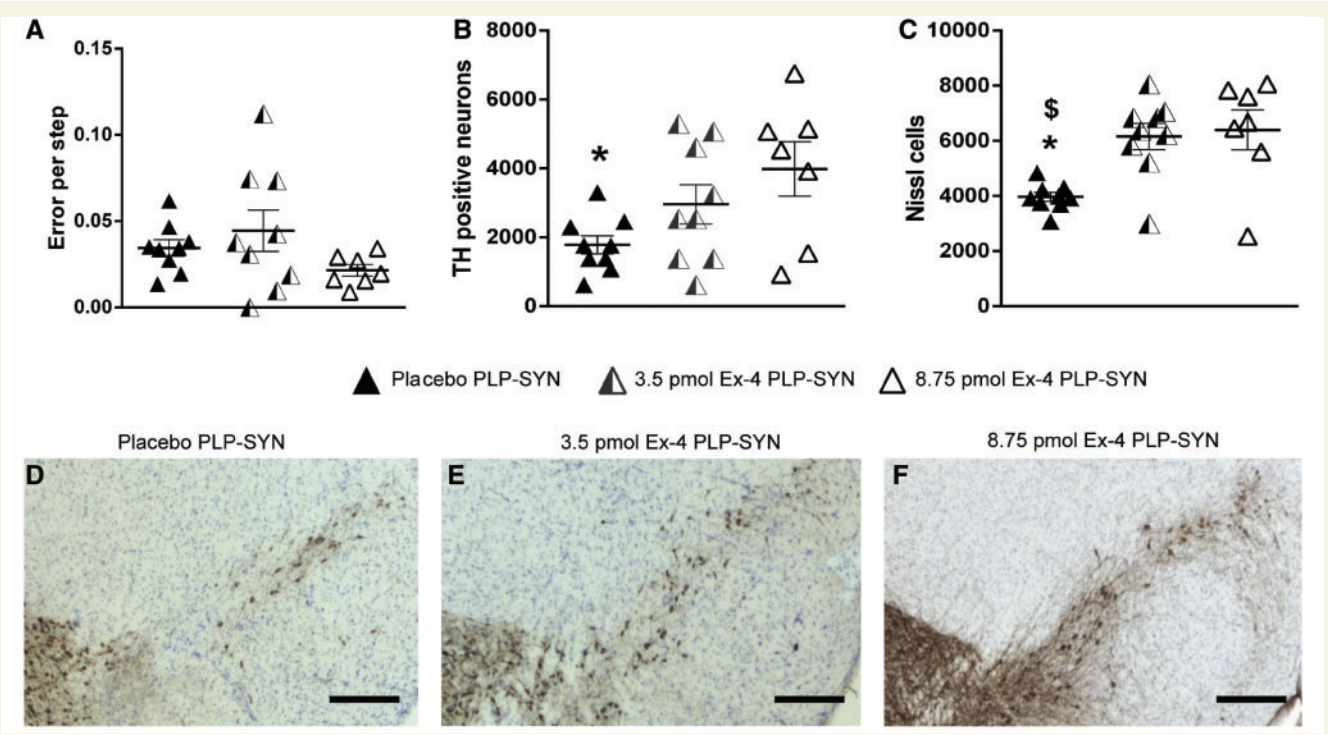

Figure 6 Exendin-4 treatment protects dopaminergic neurons in the SNc in PLP-SYN mice. (**A**) A trend for improvement of motor performance in the traversing beam task was observed in PLP-SYN mice receiving the higher dose exendin-4 treatment but the difference between groups did not reach significance. (**B**) Significant loss in tyrosine hydroxylase (TH) positive neurons in the SNc of placebo PLP-SYN mice ($n = 9$) compared to PLP-SYN mice treated with 8.75 pmol/kg/min exendin-4 ($n = 7$). (**C**) Significant loss in Nissl-stained neurons in the SNc of placebo PLP-SYN mice ($n = 9$) compared to PLP-SYN mice treated with either 3.5 pmol/kg/min ($n = 9$) or 8.75 pmol/kg/min exendin-4 ($n = 7$). (**D–F**) Representative SNc sections from placebo (**D**), 3.5 pmol/kg/min exendin-4 (**E**) and 8.75 pmol/kg/min exendin-4 treated PLP-SYN mice (**F**). Scale bar = 600 μm. A one-way ANOVA was applied to compare treatment effects of exendin-4 between groups, followed by *post hoc* Holm-Sidak tests for multiple comparisons if appropriate. If data were not normally distributed, an ANOVA on ranks was performed instead, followed by Dunn's multiple comparisons when appropriate. Values are mean ± SEM. $^{*}P < 0.05$ versus 8.75 pmol/kg/min exendin-4 PLP-SYN mice, $^{\$}P < 0.05$ versus 3.5 pmol/kg/min exendin-4 treated PLP-SYN mice.

revealed an overall significant difference in cell count in the SNc between the different groups ($H = 9.4$, $df = 2$, $P < 0.01$, Fig. 6C). *Post hoc* analysis showed that lower and higher doses of exendin-4 preserved PLP-SYN mice from SNc neuronal loss (+63%, $P < 0.05$ and +71%, $P < 0.05$, respectively, Fig. 6C).

The cytopathological hallmark of MSA is the accumulation α-synuclein aggregates in oligodendrocytes, forming GCIs. PLP-SYN mice overexpress α-synuclein under the control of the PLP promoter, leading to the formation of GCIs (Kahle *et al.*, 2002; Fernagut *et al.*, 2014*b*). We hence investigated whether exendin-4 treatment reduced α-synuclein load in the striatum of PLP-SYN mice by western blot (Fig. 7). A Kruskal-Wallis test revealed a significant difference in monomeric α-synuclein levels between groups ($H = 10.7$, $df = 2$, $P = 0.005$). *Post hoc* analysis showed that the higher dose of exendin-4 significantly decreased the quantity of monomeric α-synuclein in the striatum of PLP-SYN mice compared to placebo (−28%, $P = 0.01$) (Fig. 7A and C). *Post hoc* analysis revealed no significant effect of the lower dose of exendin-4 on monomeric α-synuclein levels in PLP-SYN mice (Fig. 7A and C). No significant differences between groups were observed for high molecular weight oligomeric species of α-synuclein (Fig. 7A and B).

Altogether, these data suggest that normalization of insulin resistance markers in PLP-SYN mice by exendin-4 treatment with the higher dose is associated with a reduction of the extent of the nigrostriatal lesion, as assessed by TH and Nissl cell counts, as well as a decrease in the α-synuclein load.

Plasma exosomal IRS-1pS307 levels correlate with readouts of neurodegeneration in treated multiple system atrophy mice

Now that insulin resistance was established in MSA and PLP-SYN mice, we sought for a peripheral biomarker. We thus measured plasma exosomal levels of IRS-1pS307 and alix in MSA mice treated with higher dose exendin-4 to determine if peripheral neural-derived markers of insulin resistance correlate with brain readouts of the

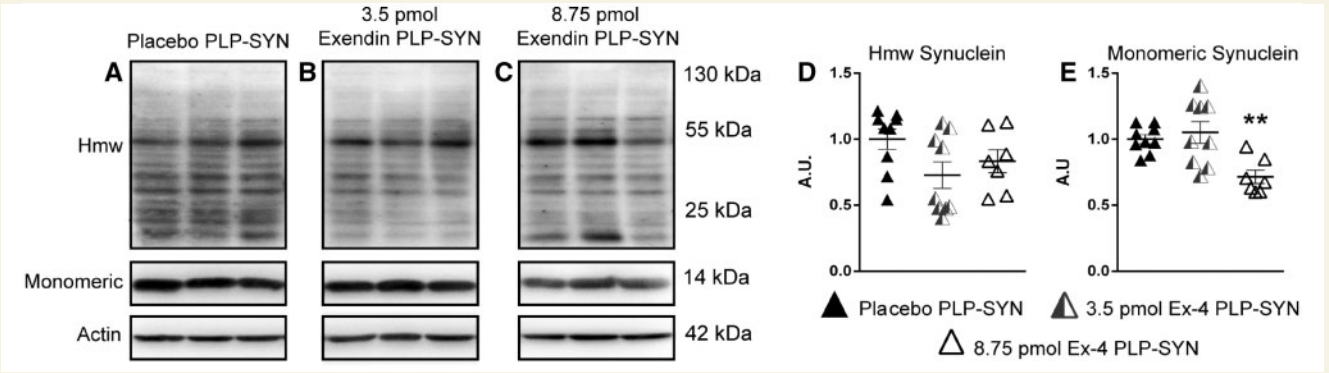

Figure 7 Exendin-4 treatment decreases α-synuclein load in the striatum of PLP-SYN. mice. (**A**) Representative western blots of high molecular weight (Hmw) oligomeric and monomeric α-synuclein in the striatum. (**B**) High molecular weight α-synuclein levels were not different between placebo ($n = 9$), 3.5 pmol/kg/min ($n = 9$) and 8.75 pmol/kg/min exendin-4 treated PLP-SYN mice ($n = 7$). (**C**) A significant decrease in monomeric α-synuclein was observed in PLP-SYN mice treated with 8.75 pmol/kg/min exendin-4 ($n = 7$) compared to placebo PLP-SYN mice ($n = 9$). A one-way ANOVA was applied to compare treatment effects of exendin-4 between groups, followed by *post hoc* Holm-Sidak tests for multiple comparisons if appropriate. If data were not normally distributed, an ANOVA on ranks was performed instead, followed by Dunn's multiple comparisons when appropriate. Values are mean ± SEM. $^{**}P < 0.01$ versus placebo PLP-SYN. A.U. = arbitrary units.

neurodegenerative process. Mean exosomal plasma levels were 451.4 ± 97.6 U/ml for IRS-1pS307 and 1150.2 ± 165.8 U/ml for alix. Normalized IRS-1pS307 values were 0.40 ± 0.09. There was a negative correlation between normalized plasma exosomal levels of IRS-1pS307 and TH ($\rho = -0.86$, $P = 0.014$) and Nissl cell counts ($\rho = -0.90$, $P = 0.005$), as well as a strong trend for striatal oligomeric α-synuclein load ($\rho = 0.75$, $P < 0.052$) (Supplementary Fig. 3), indicating that PLP-SYN mice with highest plasma exosomal IRS-1pS307 concentrations had a lower number of nigral TH and Nissl-stained neurons as well as higher striatal oligomeric α-synuclein levels. No correlation was found between plasma exosomal levels of IRS-1pS307 and monomeric α-synuclein.

Altogether, these data suggest that peripheral neural-derived exosomal IRS-1pS307/312 is a peripheral biomarker candidate that may serve as an objective outcome measure of target engagement for clinical trials with GLP-1 analogues in patients with MSA.

Discussion

Here we demonstrate insulin resistance in the brains of MSA patients as well as in a well-characterized animal model of this disease process, the PLP-SYN mouse. More specifically, the expression of IRS-1pS312 was increased in neurons and oligodendrocytes in the putamen of MSA patients compared to healthy controls, and PLP-SYN mice showed elevated IRS-1pS307 expression levels in the striatum compared to wild-type littermates. Based on these findings, we tested whether exendin-4, an FDA-approved anti-diabetic drug, would mitigate key pathological features reminiscent of MSA in PLP-SYN mice. We show that exendin-4 was capable of decreasing levels of IRS-1pS307 and IRS-1pS612. It also preserved dopaminergic neurons within the SNc and reduced monomeric α-synuclein load in the striatum in PLP-SYN mice.

Phosphorylation of IRS-1 on serine residues 312 and 616 instigates a dynamic feedback loop that negatively regulates the activity of the insulin/IGF-1 signalling pathway (Gual *et al.*, 2005; Zick, 2005). IRS-1 phosphorylation prevents its binding to insulin and IGF-1 receptors and, thereby, the activation of the insulin/IGF-1 signalling pathway, in addition to directing the receptors to the proteasome for degradation (Zick, 2001, 2005; Gual *et al.*, 2005). Increased IRS-1pS312 expression is thus considered as a marker of insulin resistance.

Neurons and oligodendrocytes are insulin-resistant in patients with multiple system atrophy

We observed severe neuronal loss in the putamen of MSA patients in accordance with the literature (Salvesen *et al.*, 2015). As almost all remaining neurons stained positive for IRS-1pS312, MSA patients had lower IRS-1pS312/S616 positive neuronal counts compared to healthy controls. Simultaneously, surviving neurons in MSA patients showed increased IRS-1pS312 staining intensity.

Insulin resistance, as assessed by enhanced phosphorylation of IRS-1 on serine residues 312, 616 and 636, has been reported in other neurodegenerative disorders and, in particular, is observed within the hippocampus in post-mortem brain tissue of patients with Alzheimer's disease and in preclinical models of Alzheimer's disease (Moloney *et al.*, 2010; Bomfim *et al.*, 2012; Talbot *et al.*, 2012). We here demonstrate altered insulin/IGF-1 signalling and insulin resistance in the putamen of MSA patients. Increased IRS-1pS616 staining in the hippocampus, midfrontal gyrus cortex and angular gyrus cortex has been reported in

patients suffering from Alzheimer's disease and tauopathies (Yarchoan *et al.*, 2014). No difference in IRS-1pS616 staining intensity was observed in the same anatomical regions in patients with MSA and Parkinson's disease, which is consistent with our observation of no difference in neuronal and oligodendroglial IRS-1pS312 staining intensity between patients with MSA and control subjects in the temporal cortex. In the present study, IRS-1pS312 and IRS-1pS616 showed a nuclear distribution in all assessed cell types in MSA patients and controls that is different from Alzheimer's disease where IRS-1pS312 staining in the temporal cortex is observed in the periphery of neurons and in extracellular thread-like structures (Moloney *et al.*, 2010). Similarly, we did find such a distribution of IRS-pS312 staining in sample cases of Alzheimer's disease that were processed together with MSA cases (data not shown). In Alzheimer's disease, IRS-1pS312 and IRS-1pS616 further co-localize with tau aggregates (Moloney *et al.*, 2010; Yarchoan *et al.*, 2014). In light of the nuclear distribution of IRS-1pS312 in MSA patients, co-localization with α-synuclein seems unlikely. No co-localization was further observed between IRS-1pS616 and α-synuclein in regions without insulin resistance in MSA patients (Yarchoan *et al.*, 2014). However, our results point to a possible relationship between the presence of α-synuclein aggregates and insulin resistance in oligodendrocytes. Future studies should assess this relation in more detail. Taken together, the findings of previous studies and our results suggest that Alzheimer's disease, tauopathies and synucleinopathies have distinct and disease-specific regional patterns of insulin resistance.

Oligodendroglia support optimal axonal function as well as survival through mechanisms both dependent and independent of myelination, and their dysfunction leads to axon degeneration and neuronal loss across several neurodegenerative diseases (Morrison *et al.*, 2013). Whereas the number of oligodendrocytes proved to be similar in MSA and healthy controls, they were insulin resistant in MSA patients compared to healthy controls, in accordance with previous studies (Ettle *et al.*, 2016). Oligodendrocyte dysfunction is believed to be of paramount importance for the pathogenesis of MSA since α-synuclein accumulates and aggregates in their cytosol (Wenning *et al.*, 2008). Whether insulin resistance precedes the formation of GCIs or is the result of α-synuclein aggregation in oligodendrocytes remains an unanswered question. Our results and *in vitro* studies support the second hypothesis as transient overexpression of α-synuclein in human neuroblastoma cells alters insulin/IGF-1 signalling and induces insulin resistance via phosphorylation of IRS-1 on serine residues (Zick, 2005; Yang *et al.*, 2013; Gao *et al.*, 2015).

Noteworthy, disease duration was correlated with insulin resistance in neurons (positive) and oligodendrocytes (negative), with an inverse relation between neuronal and oligodendroglial IRS-1pS312 staining intensity. Although the number of MSA patients in our study is small, this may suggest that oligodendroglial insulin resistance is more relevant in patients with more aggressive disease progression, while neuronal insulin resistance could predominate in patients with a slower disease course.

Insulin/IGF-1 signalling plays a prominent role in oligodendrocyte survival, proliferation, differentiation and functioning (Carson *et al.*, 1993; Zeger *et al.*, 2007). Studies have also shown that insulin/IGF-1 signalling acts as a myelin synthesis and maturation factor in several demyelinating disorders, while alteration and loss of myelin occur in MSA (Papp and Lantos, 1994; Yao *et al.*, 1995; Mason *et al.*, 2000; Song *et al.*, 2007; Ishizawa *et al.*, 2008). In this regard, mRNA and protein levels of myelin basic protein (MBP), a main constituent of myelin, are decreased. In addition, MBP degradation products accumulate in myelinated fibre bundles and oligodendrocytes in the brain of MSA patients, pointing to a possible deficit in MBP synthesis, transport and function (Song *et al.*, 2007; Salvesen *et al.*, 2015). Interestingly, IGF-1 plays a pivotal role in myelin synthesis by increasing transcripts for MBP, myelin proteolipid protein and CNPase, all known to be critical for myelin formation (Mozell and McMorris, 1991; Yao *et al.*, 1995). MSA patients also exhibit decreased levels of myelin-associated lipids that are key constituents of the myelin sheath and are implicated in myelin stability, while IGF-1 stimulates *de novo* fatty acid biosynthesis via PI3-K/Akt activation (Liang *et al.*, 2007; Don *et al.*, 2014). Early oligodendroglial dysfunction may include altered insulin/IGF-1 signalling and insulin resistance contributing to abnormal oligodendrocyte functioning and myelin alteration. As a result of compromised insulin/IGF-1 signalling in oligodendrocytes, trophic support to neurons may be compromised in MSA and contribute to degeneration of neurons that also show insulin resistance.

Microglia and astrocytes are not insulin resistant in patients with multiple system atrophy

Increased non-neuronal IRS-1pS312 and IRS-1pS616 cell counts in MSA patients were the result of the increased number of astrocytes and microglia as previously shown (Salvesen *et al.*, 2015), while a trend for decreased IRS-1pS616 expression in astrocytes was observed in MSA patients compared to controls. The significance of this trend remains unknown, bearing in mind that insulin/IGF-1 signalling in astrocytes is required for proliferation, glutamate transporter expression, glycogen synthesis and neuroprotection by decreasing oxidative stress (Heni *et al.*, 2011; Bassil *et al.*, 2014; Genis *et al.*, 2014). In this regard, glycogen, the main energy source in the brain, is almost exclusively regulated by insulin/IGF-1 signalling in astrocytes (Muhic *et al.*, 2015). Moreover, activated astrocytes produce less IGF-1 compared to naïve astrocytes, which might also lead to a decreased IGF-1 availability in the brain (Muhic *et al.*, 2015).

Insulin resistance in multiple system atrophy transgenic mice

Similar to human disease, we observed increased insulin resistance in the striatum of PLP-SYN mice, as corroborated by increased IRS-1pS307 expression. The PLP-SYN mouse is a transgenic mouse model of MSA based on the overexpression of human α-synuclein in oligodendrocytes. This model replicates several key aspects of MSA pathology, such as motor deficits, α-synuclein aggregates and SNc neuronal loss (Kahle *et al.*, 2002; Fernagut and Tison, 2012; Fernagut *et al.*, 2014*b*). We hence evaluated whether targeting insulin/IGF-1 signalling with exendin-4, a GLP-1 receptor analogue, could reverse insulin resistance in the brain and protect SNc dopaminergic neurons.

Positive effects of exendin-4 on insulin resistance and cell death but not on motor signs in multiple system atrophy mice

We here show that treatment with the higher dose of exendin-4 decreased IRS-1pS307 and IRS-1pS612 expression levels in the striatum of PLP-SYN mice. Lower levels of monomeric but not high molecular weight oligomeric α-synuclein in oligodendrocytes and preservation of dopaminergic neurons in the SNc paralleled this decrease. This observation suggests that the higher dose of exendin-4 has only modest effects on α-synuclein accumulation, insufficient to limit the aggregation of insoluble α-synuclein species. The latter are believed to be the most toxic and relevant regarding the underlying disease process (Dehay *et al.*, 2015). Interestingly, both PLP-SYN mice treated with lower or higher doses had higher numbers of Nissl positive cells compared to placebo, whereas only the higher dose group showed a significant preservation of TH-positive neurons. This suggests that the lower dose of exendin-4 allows neurons to survive, while the higher dose also improves the function of surviving dopamine neurons. Notably, following normalization of body surface area between mouse and humans, the higher dose compares favourably to the clinical dose of the once weekly form of exendin-4 (Bydureon®) used in type 2 diabetes (FDA, 2005).

We further show a correlation between plasma neural-derived IRS-1pS307 levels and readouts of cerebral cell loss and α-synuclein burden in MSA transgenic mice that were treated with the higher dose of exendin-4. This observation warrants further investigation with regard to the development of an easily accessible biomarker for MSA and a potential readout for clinical trials with GLP-1 analogues in MSA and other neurodegenerative disorders.

A trend for improvement of motor performance in the traversing beam task was observed in PLP-SYN mice receiving the higher dose exendin-4 treatment but the difference between groups did not reach significance. Differences between placebo and higher dose exendin-4 groups were similar to the significant effect of VX-765 in the same mouse model (Bassil *et al.*, 2016). The present study was underpowered to show a significant difference because of the comparison of three treatment groups instead of two. PLP-SYN mice develop progressive motor impairment in the traversing beam task, the most sensitive test to assess motor function in PLP-SYN mice (Fernagut *et al.*, 2014*b*). The motor phenotype is relatively mild over the first months of life, while the loss of dopaminergic neurons in the SNc occurs within the first 4 months of life in this model (Stefanova *et al.*, 2007). To maximize our chances to interfere with the neurodegenerative process, we opted for treating mice during the period where neuron loss occurs, which makes it less likely to see robust effects on motor dysfunction.

Previous studies have shown that exendin-4 improves motor performance and preserves dopaminergic neurons in toxin-based preclinical models of Parkinson's disease (Harkavyi *et al.*, 2008; Bassil *et al.*, 2014). However, results obtained in preclinical models based on the overexpression of α-synuclein that more closely reflect the underlying disease process in Parkinson's disease and MSA are not available. In this regard, our study provides the first *in vivo* evidence that GLP-analogues may decrease the accumulation of α-synuclein. Maintaining appropriate insulin/IGF-1 signalling in oligodendrocytes may allow the clearance systems in oligodendrocytes to better handle the overexpressed monomeric α-synuclein.

Insulin/IGF-1 signalling is pivotal to neuronal survival within the brain by modulating the activity of several pro-survival or proapoptotic effectors, such as FoxO, GSK-3β, caspases and Bcl-2 (Bassil *et al.*, 2014). The activation of insulin/IGF-1 signalling represses FoxO activity in the brain, while increased FoxO activity has been linked to apoptosis through activation of FasL promoter and Bim (Bassil *et al.*, 2014). Insulin/IGF-1 signalling is also essential for regulating axonal growth, regeneration and protein synthesis through the activation of mTOR and inhibition of GSK-3β (Bassil *et al.*, 2014). Accordingly, insulin resistance in PLP-SYN mice and MSA patients may contribute to neuronal dysfunction by decreasing the activity of prosurvival activity effectors, such as Bcl-2 and mTOR, and gene expression in neurons via decreased CREB activity (Nakamura *et al.*, 1998, 2001; Chu *et al.*, 2009; Levy *et al.*, 2009; Dehay *et al.*, 2010; Kragh *et al.*, 2013). In addition, altered insulin/IGF-1 signalling may lead to decreased repression of FoxO and caspases, thereby inducing apoptosis.

Future perspectives for developing GLP-1 analogues for treating multiple system atrophy

GLP-1 analogues are approved drugs for the treatment of type 2 diabetes and possess a good safety profile, rendering them suitable candidates for further treatment development

in MSA. In the past decade, crucial milestones have been reached for successfully conducting clinical intervention trials in patients with MSA (Fernagut *et al.*, 2014*a*). Similarly, positive findings of preclinical proof-of-concept studies have already been translated into early phase clinical trials in Alzheimer's disease and Parkinson's disease assessing the safety and efficacy of the GLP-1 analogues, exendin-4 and liraglutide. Such translation should now be extended to MSA.

Conclusion

In conclusion, we here show insulin resistance in the putamen of MSA patients as evidenced by increased IRS-1pS312 expression, notably in neurons and oligodendrocytes. Abnormal insulin/IGF-1 signalling in oligodendrocytes may lead to impaired oligodendrocyte functioning, thereby contributing to secondary neurodegeneration in the putamen of MSA patients. PLP-SYN mice likewise show impaired insulin/IGF-1 signalling in the striatum. Alterations of insulin/IGF-1 signalling were reversed by clinically translatable doses of exendin-4 treatment in PLP-SYN mice. Moreover, exendin-4 treatment preserved dopaminergic neurons of the SNc and decreased monomeric α-synuclein concentrations. This proof-of-concept preclinical study together with the data showing insulin resistance in the brain of MSA patients provides a rationale for the development of GLP-1 analogues as a potential neuroprotective treatment for MSA.

Acknowledgements

The authors thank Dr Elisabeth Normand, Melissa Deshors and Anaelle Le Bris for animal care, as well as the GIE Neuro-CEB, Paris, France, for contributing tissue samples. The microscopy was done at the Bordeaux Imaging Center, a service unit of the CNRS-INSERM and Bordeaux University, member of the national infrastructure France BioImaging. The Université de Bordeaux, the Centre National de la Recherche Scientifique and the Intramural Research Program of the National Institute on Aging, NIH, provided infrastructural support.

Funding

This work was in part supported by the MSA Coalition (grant to W.G.M.) and grant LABEX BRAIN ANR-10-LABX-43. The funders had no role in study design, data collection and analysis, decision to publish, or preparation of the manuscript.

Supplementary material

Supplementary material is available at *Brain* online.

References

Aviles-Olmos I, Dickson J, Kefalopoulou Z, Djamshidian A, Ell P, Soderlund T, et al. Exenatide and the treatment of patients with Parkinson's disease. J Clin Invest 2013; 123: 2730–6.

Aviles-Olmos I, Dickson J, Kefalopoulou Z, Djamshidian A, Kahan J, Ell P, et al. Motor and cognitive advantages persist 12 months after exenatide exposure in Parkinson's disease. J Parkinsons Dis 2014; 4: 337–44.

Bassil F, Fernagut PO, Bezard E, Meissner WG. Insulin, IGF-1 and GLP-1 signaling in neurodegenerative disorders: targets for disease modification?. Prog Neurobiol 2014; 118: 1–18.

Bassil F, Fernagut PO, Bezard E, Pruvost A, Leste-Lasserre T, Hoang QQ, et al. Reducing C-terminal truncation mitigates synucleinopathy and neurodegeneration in a transgenic model of multiple system atrophy. Proc Natl Acad Sci USA 2016; 113: 9593–8.

Bomfim TR, Forny-Germano L, Sathler LB, Brito-Moreira J, Houzel JC, Decker H, et al. An anti-diabetes agent protects the mouse brain from defective insulin signaling caused by Alzheimer's disease- associated Abeta oligomers. J Clin Invest 2012; 122: 1339–53.

Carson MJ, Behringer RR, Brinster RL, McMorris FA. Insulin-like growth factor I increases brain growth and central nervous system myelination in transgenic mice. Neuron 1993; 10: 729–40.

Chu Y, Dodiya H, Aebischer P, Olanow CW, Kordower JH. Alterations in lysosomal and proteasomal markers in Parkinson's disease: relationship to alpha-synuclein inclusions. Neurobiol Dis 2009; 35: 385–98.

Dehay B, Bourdenx M, Gorry P, Przedborski S, Vila M, Hunot S, et al. Targeting alpha-synuclein for treatment of Parkinson's disease: mechanistic and therapeutic considerations. Lancet Neurol 2015; 14: 855–66.

Dehay B, Bove J, Rodriguez-Muela N, Perier C, Recasens A, Boya P, et al. Pathogenic lysosomal depletion in Parkinson's disease. J Neurosci 2010; 30: 12535–44.

Don AS, Hsiao JH, Bleasel JM, Couttas TA, Halliday GM, Kim WS. Altered lipid levels provide evidence for myelin dysfunction in multiple system atrophy. Acta Neuropathol Commun 2014; 2: 150.

Ettle B, Kerman BE, Valera E, Gillmann C, Schlachetzki JC, Reiprich S, et al. alpha-Synuclein-induced myelination deficit defines a novel interventional target for multiple system atrophy. Acta Neuropathol 2016; 132: 59–75.

FDA. Estimating the safe starting dose in clinical trials for therapeutics in adult healthy volunteers, Center for Drug Evaluation and Research and Center for Biologics Evaluation and Research 2005. Available from: http://www.fda.gov/downloads/Drugs/. . ./Guidances/UCM078932.pdf

Fernagut PO, Dehay B, Maillard A, Bezard E, Perez P, Pavy-Le Traon A, et al. Multiple system atrophy: a prototypical synucleinopathy for disease-modifying therapeutic strategies. Neurobiol Dis 2014a; 67: 133–9.

Fernagut PO, Hutson CB, Fleming SM, Tetreaut NA, Salcedo J, Masliah E, et al. Behavioral and histopathological consequences of paraquat intoxication in mice: effects of alpha-synuclein over-expression. Synapse 2007; 61: 991–1001.

Fernagut PO, Meissner WG, Biran M, Fantin M, Bassil F, Franconi JM, et al. Age-related motor dysfunction and neuropathology in a transgenic mouse model of multiple system atrophy. Synapse 2014b; 68: 98–106.

Fernagut PO, Tison F. Animal models of multiple system atrophy. Neuroscience 2012; 211: 77–82.

Fiandaca MS, Kapogiannis D, Mapstone M, Boxer A, Eitan E, Schwartz JB, et al. Identification of preclinical Alzheimer's disease by a profile of pathogenic proteins in neurally derived blood exosomes: a case-control study. Alzheimers Dement 2015; 11: 600–7.e1.

Fleming SM, Salcedo J, Fernagut PO, Rockenstein E, Masliah E, Levine MS, et al. Early and progressive sensorimotor anomalies in

mice overexpressing wild-type human alpha-synuclein. J Neurosci 2004; 24: 9434–40.

Gao S, Duan C, Gao G, Wang X, Yang H. Alpha-synuclein overexpression negatively regulates insulin receptor substrate 1 by activating mTORC1/S6K1 signaling. Int J Biochem Cell Biol 2015; 64: 25–33.

Genis L, Davila D, Fernandez S, Pozo-Rodrigalvarez A, Martinez-Murillo R, Torres-Aleman I. Astrocytes require insulin-like growth factor I to protect neurons against oxidative injury. F1000Res 2014; 3: 28.

Gilman S, Wenning GK, Low PA, Brooks DJ, Mathias CJ, Trojanowski JQ, et al. Second consensus statement on the diagnosis of multiple system atrophy. Neurology 2008; 71: 670–6.

Goetzl EJ, Boxer A, Schwartz JB, Abner EL, Petersen RC, Miller BL, et al. Altered lysosomal proteins in neural-derived plasma exosomes in preclinical Alzheimer disease. Neurology 2015; 85: 40–7.

Gual P, Le Marchand-Brustel Y, Tanti JF. Positive and negative regulation of insulin signaling through IRS-1 phosphorylation. Biochimie 2005; 87: 99–109.

Harkavyi A, Abuirmeileh A, Lever R, Kingsbury AE, Biggs CS, Whitton PS. Glucagon-like peptide 1 receptor stimulation reverses key deficits in distinct rodent models of Parkinson's disease. J Neuroinflammation 2008; 5: 19.

Heni M, Hennige AM, Peter A, Siegel-Axel D, Ordelheide AM, Krebs N, et al. Insulin promotes glycogen storage and cell proliferation in primary human astrocytes. PLoS One 2011; 6: e21594.

Ishizawa K, Komori T, Arai N, Mizutani T, Hirose T. Glial cytoplasmic inclusions and tissue injury in multiple system atrophy: a quantitative study in white matter (olivopontocerebellar system) and gray matter (nigrostriatal system). Neuropathology 2008; 28: 249–57.

Jafferali S, Dumont Y, Sotty F, Robitaille Y, Quirion R, Kar S. Insulin-like growth factor-I and its receptor in the frontal cortex, hippocampus, and cerebellum of normal human and alzheimer disease brains. Synapse 2000; 38: 450–9.

Kahle PJ, Neumann M, Ozmen L, Muller V, Jacobsen H, Spooren W, et al. Hyperphosphorylation and insolubility of alpha-synuclein in transgenic mouse oligodendrocytes. EMBO Rep 2002; 3: 583–8.

Kapogiannis D, Boxer A, Schwartz JB, Abner EL, Biragyn A, Masharani U, et al. Dysfunctionally phosphorylated type 1 insulin receptor substrate in neural-derived blood exosomes of preclinical Alzheimer's disease. FASEB J 2015; 29: 589–96.

Kragh CL, Fillon G, Gysbers A, Hansen HD, Neumann M, Richter-Landsberg C, et al. FAS-dependent cell death in alpha-synuclein transgenic oligodendrocyte models of multiple system atrophy. PLoS One 2013; 8: e55243.

Levy OA, Malagelada C, Greene LA. Cell death pathways in Parkinson's disease: proximal triggers, distal effectors, and final steps. Apoptosis 2009; 14: 478–500.

Li Y, Perry T, Kindy MS, Harvey BK, Tweedie D, Holloway HW, et al. GLP-1 receptor stimulation preserves primary cortical and dopaminergic neurons in cellular and rodent models of stroke and Parkinsonism. Proc Natl Acad Sci USA 2009; 106: 1285–90.

Liang G, Cline GW, Macica CM. IGF-1 stimulates *de novo* fatty acid biosynthesis by Schwann cells during myelination. Glia 2007; 55: 632–41.

Mason JL, Ye P, Suzuki K, D'Ercole AJ, Matsushima GK. Insulin-like growth factor-1 inhibits mature oligodendrocyte apoptosis during primary demyelination. J Neurosci 2000; 20: 5703–8.

Moloney AM, Griffin RJ, Timmons S, O'Connor R, Ravid R, O'Neill C. Defects in IGF-1 receptor, insulin receptor and IRS-1/2 in Alzheimer's disease indicate possible resistance to IGF-1 and insulin signalling. Neurobiol Aging 2010; 31: 224–43.

Morrison BM, Lee Y, Rothstein JD. Oligodendroglia: metabolic supporters of axons. Trends Cell Biol 2013; 23: 644–51.

Mozell RL, McMorris FA. Insulin-like growth factor I stimulates oligodendrocyte development and myelination in rat brain aggregate cultures. J Neurosci Res 1991; 30: 382–90.

Muhic M, Vardjan N, Chowdhury HH, Zorec R, Kreft M. Insulin and Insulin-like Growth Factor 1 (IGF-1) modulate cytoplasmic glucose and glycogen levels but not glucose transport across the membrane in astrocytes. J Biol Chem 2015; 290: 11167–76.

Nakamura S, Kawamoto Y, Kitajima K, Honjo Y, Matsuo A, Nakano S, et al. Immunohistochemical localization of phosphoinositide 3-kinase in brains with multiple system atrophy. Clin Neuropathol 2001; 20: 243–7.

Nakamura S, Kawamoto Y, Nakano S, Akiguchi I, Kimura J. Cyclin-dependent kinase 5 and mitogen-activated protein kinase in glial cytoplasmic inclusions in multiple system atrophy. J Neuropathol Exp Neurol 1998; 57: 690–8.

Numao A, Suzuki K, Miyamoto M, Miyamoto T, Hirata K. Clinical correlates of serum insulin-like growth factor-1 in patients with Parkinson's disease, multiple system atrophy and progressive supranuclear palsy. Parkinsonism Relat Disord 2014; 20: 212–6.

Ozawa T, Paviour D, Quinn NP, Josephs KA, Sangha H, Kilford L, et al. The spectrum of pathological involvement of the striatonigral and olivopontocerebellar systems in multiple system atrophy: clinicopathological correlations. Brain 2004; 127 (Pt 12): 2657–71.

Papp MI, Lantos PL. The distribution of oligodendroglial inclusions in multiple system atrophy and its relevance to clinical symptomatology. Brain 1994; 117 (Pt 2): 235–43.

Pellecchia MT, Pivonello R, Longo K, Manfredi M, Tessitore A, Amboni M, et al. Multiple system atrophy is associated with changes in peripheral insulin-like growth factor system. Mov Disord 2010; 25: 2621–6.

Salvesen L, Ullerup BH, Sunay FB, Brudek T, Lokkegaard A, Agander TK, et al. Changes in total cell numbers of the basal ganglia in patients with multiple system atrophy—a stereological study. Neurobiol Dis 2015; 74: 104–13.

Schechter R, Beju D, Gaffney T, Schaefer F, Whetsell L. Preproinsulin I and II mRNAs and insulin electron microscopic immunoreaction are present within the rat fetal nervous system. Brain Res 1996; 736: 16–27.

Schwarz SC, Seufferlein T, Liptay S, Schmid RM, Kasischke K, Foster OJ, et al. Microglial activation in multiple system atrophy: a potential role for NF-kappaB/rel proteins. Neuroreport 1998; 9: 3029–32.

Song YJ, Lundvig DM, Huang Y, Gai WP, Blumbergs PC, Hojrup P, et al. p25alpha relocalizes in oligodendroglia from myelin to cytoplasmic inclusions in multiple system atrophy. Am J Pathol 2007; 171: 1291–303.

Stefanova N, Reindl M, Neumann M, Haass C, Poewe W, Kahle PJ, et al. Oxidative stress in transgenic mice with oligodendroglial alpha-synuclein overexpression replicates the characteristic neuropathology of multiple system atrophy. Am J Pathol 2005; 166: 869–76.

Stefanova N, Reindl M, Neumann M, Kahle PJ, Poewe W, Wenning GK. Microglial activation mediates neurodegeneration related to oligodendroglial alpha-synucleinopathy: implications for multiple system atrophy. Mov Disord 2007; 22: 2196–203.

Talbot K, Wang HY, Kazi H, Han LY, Bakshi KP, Stucky A, et al. Demonstrated brain insulin resistance in Alzheimer's disease patients is associated with IGF-1 resistance, IRS-1 dysregulation, and cognitive decline. J Clin Invest 2012; 122: 1316–38.

Ubhi K, Rockenstein E, Mante M, Inglis C, Adame A, Patrick C, et al. Neurodegeneration in a transgenic mouse model of multiple system atrophy is associated with altered expression of oligodendroglial-derived neurotrophic factors. J Neurosci 2010; 30: 6236–46.

Wenning GK, Stefanova N, Jellinger KA, Poewe W, Schlossmacher MG. Multiple system atrophy: a primary oligodendrogliopathy. Ann Neurol 2008; 64: 239–46.

Yang W, Wang X, Duan C, Lu L, Yang H. Alpha-synuclein overexpression increases phospho-protein phosphatase 2A levels via formation of calmodulin/Src complex. Neurochem Int 2013; 63: 180–94.

Yao DL, Liu X, Hudson LD, Webster HD. Insulin-like growth factor I treatment reduces demyelination and up-regulates gene expression of myelin-related proteins in experimental autoimmune encephalomyelitis. Proc Natl Acad Sci USA 1995; 92: 6190–4.

Yarchoan M, Toledo JB, Lee EB, Arvanitakis Z, Kazi H, Han LY, et al. Abnormal serine phosphorylation of insulin receptor substrate 1 is associated with tau pathology in Alzheimer's disease and tauopathies. Acta Neuropathol 2014; 128: 679–89.

Zeger M, Popken G, Zhang J, Xuan S, Lu QR, Schwab MH, et al. Insulin-like growth factor type 1 receptor signaling in the cells of oligodendrocyte lineage is required for normal *in vivo* oligodendrocyte development and myelination. Glia 2007; 55: 400–11.

Zick Y. Insulin resistance: a phosphorylation-based uncoupling of insulin signaling. Trends Cell Biol 2001; 11: 437–41.

Zick Y. Ser/Thr phosphorylation of IRS proteins: a molecular basis for insulin resistance. Sci STKE 2005; 2005: pe4.